https://doi.org/10.5194/egusphere-2026-1118
Preprint. Discussion started: 27 March 2026

Non-Maxwellian electron distributions in the D region during artificial heating (Paper II): Electron cooling rates

Margaretha Myrvang[1] and Björn Gustavsson[1]

[1]UiT The Arctic University of Norway, Department of Physics and Technology, Postboks 6050 Langnes, 9037 Tromsø

Correspondence: Margaretha Myrvang (mmy002@uit.no)

Abstract. This paper investigates how non-Maxwellian distributions of heated electrons modify the macroscopic properties of the electron gas in the D region. Adjusted electron cooling rates for vibrational excitation of molecular nitrogen and molecular oxygen, as well as excitation of fine structure levels in atomic oxygen, are presented. These electron cooling rates are compared to Maxwellian cooling rates from previous studies by Pavlov (1998a); Campbell et al. (2004), Pavlov (1998b) and Pavlov and Berringston (1999). We find that the electron cooling rates for vibrational excitation of molecular nitrogen and excitation of fine structure levels in atomic oxygen are more affected by deviations from Maxwellian compared to the cooling rates for vibrational excitation of molecular oxygen. This is due changes in the electron phase space density, where inelastic collision between electrons and neutrals leads to redistribution of electrons.

1 Introduction

Electron cooling rates, where electrons transfer some of their kinetic energy through collisions with neutrals and ions, are an important factor for the energy balance in the ionosphere. Previously, electron cooling rates have typical been calculated under the assumption that the electron distributions are Maxwellian. This assumption simplifies calculations significantly, and allows for the computation of analytical expression (Stubbe and Varnum, 1972; Pavlov, 1998a, b; Pavlov and Berringston, 1999; Jones et al., 2003). However, in the lower ionosphere, the deviation from a Maxwellian can have a significant impact on the electron cooling rates due to the high densities of molecular nitrogen N_2 and molecular oxygen O_2.

In the lower part of the ionosphere, the ionization fraction is typical very small: $N_e/N_n \approx 10^{-8} - 10^{-10}$, and the collision frequency is much higher than the plasma and gyro-frequency. As a consequence, the electron distribution can deviate significantly from a Maxwellian due to inelastic collisions, as shown by for example Carleton and Megill (1962); Mintzer (1964); Gurevich (1978); Stubbe (1981); Gustavsson et al. (2004), and by Myrvang et al., referred to hereafter as paper I. An important factor contributing to the deviation from a Maxwellian is the excitation of vibrational states of N_2, which have large cross section between 2-3.5 eV, as shown in Paper I. These deviations from a Maxwellian affect the macroscopic properties of the D region electron gas, such as electron cooling and heating rates, refractive index, electron-neutral collision frequency and absorption of radio wave energy. Accurate electron cooling rates, heat conductivity and related parameters, are necessary to model the ionospheric response to internal and external forcing. Examples of ionospheric modelling include Belova et al. (1995); Kassa et al. (2005); Kero et al. (2000, 2007); Myrvang et al. (2021).

https://doi.org/10.5194/egusphere-2026-1118
Preprint. Discussion started: 27 March 2026

This paper (paper II) is the second in a series of two papers that address the influence of non-Maxwellian electron distributions on the D region electron gas. In this paper, we study how the non-Maxwellian distribution impacts electron cooling rates. The aim is to compute electron cooling rates using the non-Maxwellian distributions from Paper I and compare them to previous works by Pavlov (1998a); Campbell et al. (2004) for vibrational excitation of N_2, Pavlov (1998b) for vibrational excitation of O_2 and Pavlov and Berringston (1999) for excitation of fine structure levels in atomic oxygen O. These calculations are performed using cross section from Campbell et al. (2004) for vibrational excitation of N_2, Allen (1995) for vibrational excitation of O_2 and Bell et al. (1998) for excitation of fine structure levels in O.

We present cooling rates correction factors that account for the deviation between non-Maxwellian and Maxwellian distributions, as well as an empirical relation between heat absorbed by the electron gas and the second moment temperature for non-Maxwellian distribution in the D region. The correction factors are expressed as the ratio between non-Maxwellian and Maxwellian cooling rates. These ratio can be used as corrections factor for Pavlov's analytical cooling rates for Maxwellian distributions, which were based on the best available cross sections in 1998-1999, to align with the cooling rates computed in this work for non-Maxwellian distributions using the best available cross sections we were able to find.

2 Theory

2.1 Rate coefficients

To compare cooling rates for electrons with non-Maxwellian and Maxwellian distributions, expressions for the rate coefficients, K, are needed. For electrons and neutrals with velocity distributions $f_e(\boldsymbol{v_e})$, $f_N(\boldsymbol{v_N})$, respectively, the general form of K is given by the collision integral (e.g., Rees, 1989, p.69):

$$K = \int \boldsymbol{v_{eN}}\sigma(v_e)f_e(\boldsymbol{v_e})f_N(\boldsymbol{v_N})d\boldsymbol{v_e}d\boldsymbol{v_N} = \int \boldsymbol{v_e}\sigma(v_e)f_e(\boldsymbol{v_e})f_N(\boldsymbol{v_N})d\boldsymbol{v_e}d\boldsymbol{v_N} \tag{1}$$

The relative velocity between electrons and neutrals $\boldsymbol{v_{eN}}$ can be replaced with the electron velocity $\boldsymbol{v_e}$, since electrons move much faster than the neutrals. For Maxwellian distribution, the rate coefficients becomes:

$$K(T_e) = \sqrt{\frac{8}{\pi m_e}}\frac{1}{(k_B T_e)^{3/2}}\int_0^\infty \sigma(E)E\exp\left(-\frac{E}{k_B T_e}\right)dE \tag{2}$$

This expression is derived after a change of variable from velocity to energy, $E = \frac{1}{2}m_e v^2$, where k_B is Boltzmann constant, m_e is the electron mass, $\sigma(E)$ is cross sections and T_e is the electron temperature. When heat is added to the electron gas, for example by high power high frequency radio wave with angular frequency ω and amplitude electrical fields E_0, it is possible to calculate the electron distribution, as described in Paper I. For such distributions, the same procedure leads to rate coefficient for the corresponding energy distribution:

$$K(T_e) = \frac{8\pi}{m_e^2}A\int_0^\infty \sigma(E)E\exp\left\{-\int_0^{v_e'}\frac{m_e v_e + \dfrac{m_e^2 G(v_e)}{4\sigma_0 B_0 v_e f_0(v_e)}}{k_b T_n + \dfrac{m_e^2 b r_N \gamma^2}{24\sigma_0 B_0}\dfrac{v_e^3}{\omega^2+\nu^2}}dv_e\right\}dE \tag{3}$$

https://doi.org/10.5194/egusphere-2026-1118
Preprint. Discussion started: 27 March 2026

where E is the energy with speed v_e', γ is $-q_e E_0/m_e$ with $-q_e$ as the elementary charge of an electron and , T_n is the neutral temperature, ν is the electron-neutral collision frequency, $\sigma_0 B_0 = 2.49 \cdot 10^{21}$ kg $\cdot$ m$^4 \cdot$ s^{-2} and $b = 2.8 \cdot 10^{-25}$ m $\cdot$ s, $r_N = N_n/N_{n2}$ with $N_n = N_2 + O_2 + O$ and $N_{n2} = N_2 + O_2$, which are the number density of N_2, O_2 or O, and A is the normalization constant. The normalization constant A is found by conserving the electron density N_e:

$$A = \frac{N_e}{4\pi \int_0^\infty f_0(v) v^2 dv} \tag{4}$$

2.2 Cooling rates from Boltzmann equation

The electron cooling rates represents the energy loss of electrons during collisions with neutrals. In these collisions, electrons at all energies collide with atoms, molecules and ions, losing energy corresponding to the excitation energy of each neutral species and excitation state. As such, in our solution of the Boltzmann equation, the contribution to the inelastic collisions integral $(\partial f_0/\partial t)_{ie}$ for each excitation is calculated as described in Eq. 9 from Paper I. This approach provides a direct method to calculate the electron cooling rates, explicitly representing the total energy loss of the electron gas for each excitation process. This allows us to compute the cooling effects due to vibrational excitation of N_2 and O_2, fine structure levels in O and electronic excitation of $O_2(a^1\Delta_g)$, $O_2(b^1\Sigma_g^+)$, $O(^1D)$ and $O(^1S)$. By directly applying this method to the vibrational excitation of N_2 and O_2, we obtain the same results as those derived from Eq. 6 and Eq. 7, respectively.

2.3 Electron temperature

In order to compare cooling rates for non-Maxwellian and Maxwellian distributions, a suitable electron temperature needs to chosen for the Maxwellian distribution. The seemingly most obvious choice is to assign the Maxwellian distribution the same second moment as the non-Maxwellian distribution, that is, to set the Maxwellian temperature equal to the second moment temperature $T_{2\text{nd}}$, as described in Paper I. However, we will show that this approach leads to an excessively large total cooling of the Maxwellian distribution. A physically more reasonable approach is to utilize the electron energy equation (e.g., Shoucri and Morales, 1984; Hansen et al., 1992; Gustavsson et al., 2010). At steady state, under D region conditions where time variation, advection and convection of heat are negligible, the energy equation simplifies to a balance between local heating and cooling (Schunk and Nagy, 1978; Kero et al., 2000):

$$Q(T_e) - L(T_e) = 0 \tag{5}$$

Here, L represents the sum of all cooling rates and Q is the absorbed power. Using Eq. 5 to determine the temperature, refereed to hereafter as T_L, provides a Maxwellian distribution that absorbs the same amount of heat as the non-Maxwellian distribution. We use analytical expressions from Pavlov (1998a, b); Pavlov and Berringston (1999) for the Maxwellian cooling rates. However, it is important to note that these Maxwellian distributions do not contain the same amount of thermal energy as the corresponding non-Maxwellian distributions.

https://doi.org/10.5194/egusphere-2026-1118
Preprint. Discussion started: 27 March 2026

2.4 Cooling rates for vibrational excitation of N_2 and O_2

For the electron cooling rates of vibrational excitation of N_2 and O_2, we only consider the transition from the vibrational ground state, since the number density of vibrationally exited N_2 and O_2 is small, and their contribution to electron cooling is negligible (Pavlov, 1998a, b). In addition, we assume that the vibrational temperature T_{vib} is equal to the neutral temperature T_n. With these assumptions, the electron cooling rate is given by:

$$L_{vib}(N_2) = N_e N_2 \{1 - \exp(-E_1/k_b T_n)\} \sum_{v=1}^{10} Q\{1 - \exp[vE_1(k_b T_e^{-1} - k_b T_n^{-1})]\} \tag{6}$$

for vibrational excitation of N_2 from the ground state $v = 0$, adapted from Eq. 11 in Pavlov (1998a), and:

$$L_{vib}(O_2) = N_e O_2 \sum_{v=1}^{7} Q\{1 - \exp[vE_1'(k_b T_e^{-1} - k_b T_n^{-1})]\} \tag{7}$$

for vibrational excitation of O_2 from the ground state $v = 0$, adapted from Eq. 8 in Pavlov (1998b). In both Eq. 6 and 7, v is the vibrational level, N_e is the electron number density, E_1 is the energy of the first vibrational level with $E_1 = 0.2889$ eV for N_2 and $E_1' = 0.1929$ eV for O_2. Furthermore, for both neutral species Q is defined as:

$$Q = E_v K(T_e) \tag{8}$$

Here, $K(T_e)$ is the rate coefficient as given by Eq. 2 for a Maxwellian distribution and Eq. 3 for a non-Maxwellian distribution. Note that Q in Eq. 8 is the same as Q_{0v} in Pavlov (1998a) and Pavlov (1998b). The energy E_v of the vibrational level v is approximately:

$$E_v = vE_1' - v(v-1)\Delta E' \tag{9}$$

for vibrational excitation of O_2, where $\Delta E' = 0.0015$ eV for O_2. We take values of E_v for vibrational excitation of N_2 from table 2.1 in Itikawa et al. (1986).

2.5 Rotational cooling rates

To compute non-Maxwellian cooling rates for rotational excitation of N_2 and O_2, we use the general expression for inelastic collisions from Eq. 1 in Stubbe and Varnum (1972):

$$L_{rot} = N_e N_l \frac{1}{Z} \sum_{i=0}^{m-1} \sum_{j=i+1}^{m} \Delta E_{ij} K(T_e) g_i \exp\left(-\frac{E_i}{k_b T_n}\right) \left(\exp\left[-\frac{\Delta E_{ij}}{k_b T_e T_n}(T_e - T_n) - 1\right]\right) \tag{10}$$

for the neutral constituents N_l, and where E_i is the energy of the i^{th} state of the neutral, $\Delta E_{ij} = E_j - E_i$, E_j is the energy of the j^{th} state of the neutral, m is the number of energy states of the neutral, $Z = \sum_{j=0}^{\infty} g_j \exp(-E_j/k_b T_n)$ is the partition function, g_i is the statistical weight of the i^{th} state, g_j is the statistical weight of the j^{th} state and $K(T_e)$ is given in Eq. 3. For rotational excitation of N_2 and O_2, we consider several transitions from Schmalzried et al. (2023); Takayanagi and Itikawa (1970); Itikawa et al. (2006). Values of g_i, g_j, E_{ij}, E_i and E_j are taken from Schmalzried et al. (2023). Maxwellian cooling rates for rotational excitation of N_2 or O_2 are from Pavlov (1998a) and Pavlov (1998a), respectively.

https://doi.org/10.5194/egusphere-2026-1118
Preprint. Discussion started: 27 March 2026

3 Cooling rates for excitation of vibrational states of N_2 and O_2 and fine structure of O

We compute the electron cooling rates using neutral densities and temperatures from MSISE-90 model (Hedin, 1991; Picone et al., 2002), and electron density from an ionospheric model by Baumann et al. (2013). Table 1 presents the electron densities, neutral densities and neutral temperatures used in this study for the altitudes of 70, 80, 90 and 100 km.

Table 1. Electron densities, neutral densities and neutral temperatures used in this study for the altitudes of 70, 80, 90 and 100 km.

Height	N_e $[m^{-3}]$	N_2 $[m^{-3}]$	O_2 $[m^{-3}]$	O $[m^{-3}]$	T_n $[K]$
70 km	$1.29 \cdot 10^5$	$1.34 \cdot 10^{21}$	$3.55 \cdot 10^{20}$	0	222
80 km	$1.03 \cdot 10^7$	$8.03 \cdot 10^{19}$	$3.10 \cdot 10^{20}$	$1.64 \cdot 10^{15}$	190
90 km	$1.33 \cdot 10^9$	$5.32 \cdot 10^{19}$	$1.31 \cdot 10^{19}$	$1.17 \cdot 10^{17}$	173
100 km	$2.14 \cdot 10^9$	$7.63 \cdot 10^{18}$	$1.67 \cdot 10^{18}$	$1.81 \cdot 10^{17}$	195

Electron cooling rates Q for vibrational excitation of N_2 and O_2, as well as for excitation of fine structure levels in O, are shown in Fig. 1, Fig. 2 and Fig. 3, receptively, as a function of electric field (E_0) for altitudes of 70, 80, 90 and 100 km. Non-Maxwellian Q values are shown as blue solid lines, while Maxwellian Q values are shown as blue dashed-dotted lines. The temperature of the Maxwellian distribution, depicted as red solid lines, corresponds to the second moment temperature T_{2nd} of the associated non-Maxwellian distribution. For vibrational excitation of N_2 in Fig. 1, the discrepancy between the non-Maxwellian and Maxwellian Q varies with height and electric field. At 70 km, the non-Maxwellian Q is slightly lower than the Maxwellian Q for electric fields above approximately 1 V/m. However, overall, Q for both distributions are quite similar. At altitudes of 80, 90 and 100 km, the non-Maxwellian Q is higher than the Maxwellian Q for electric fields below 2 V/m and consistently lower for electric fields above 2 V/m. Notably,at 80 km the non-Maxwellian Q is only slightly higher below 2 V/m compared to 90 and 100 km. We find that the non-Maxwellian and Maxwellian Q for vibrational excitation of O_2 in Fig. 2 are generally similar at 70, 80, 90 and 100 km. However, at 80, 90 and 100 km, non-Maxwellian Q is slightly higher than the Maxwellian Q for electric fields below approximately 1.5 V/m. The results in Fig. 3 for excitation of fine structure levels in O, show that the electron cooling rates Q are zero at 70 km, while at 80, 90 and 100 km, the non-Maxwellian Q are higher than the Maxwellian Q, except at 90 km for electric field below 1 V/m.

To understand why the discrepancy between the non-Maxwellian and Maxwellian Q for vibrational excitation of N_2 varies with electric field, we consider the deviations of the distribution from Maxwellian and the electron temperature T_{2nd}, both of which are important factors. As shown in Paper I, the non-Maxwellian distribution exhibits a sharp fall-off at around 2 eV due to the vibrational excitation of N_2, which redistributes electrons to energies below 2 eV, thereby increasing the phase space density in this energy range. This effective cut-off is primarily caused by the large cross sections of vibrational excitation of N_2 in the energy range of 2-3.5 eV. The cut-off at 2 eV becomes more pronounced with higher electric fields, as electrons are increasingly more likely to excite vibrational states in N_2 and degrade to lower energies as more energy is supplied to the electron gas. Paper I also show that the redistribution of electrons to energies below 2 eV due to the cut-off leads to an increase

https://doi.org/10.5194/egusphere-2026-1118
Preprint. Discussion started: 27 March 2026

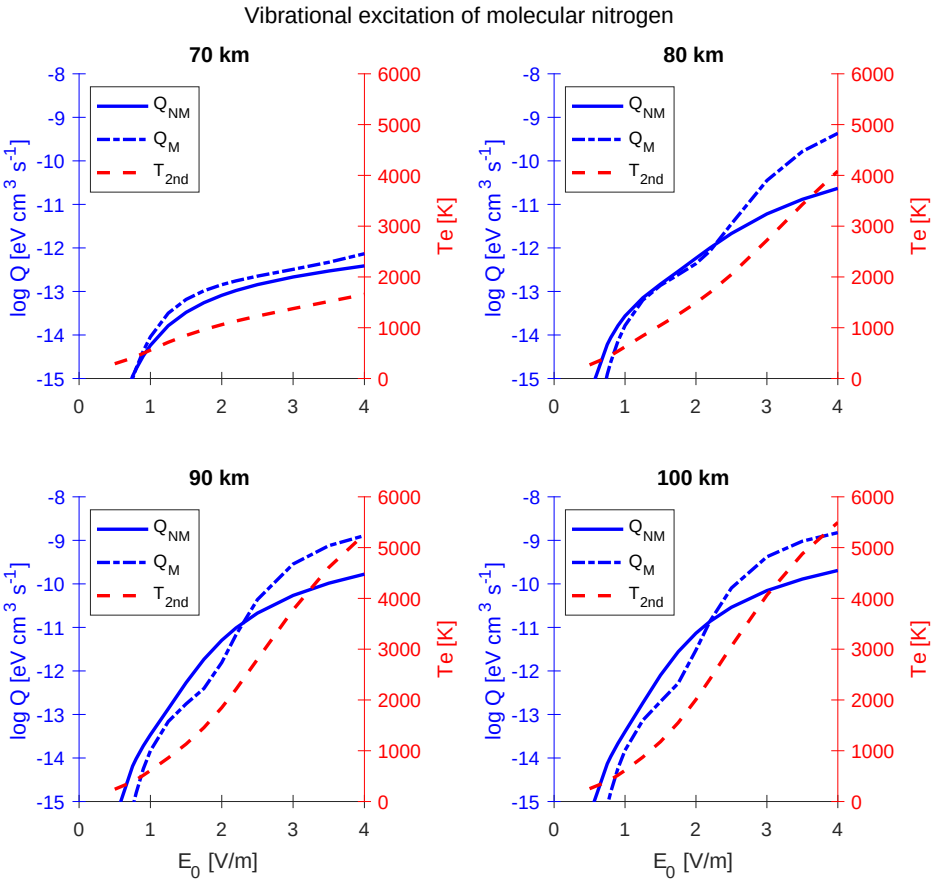

Figure 1. $\log_{10} Q$ for vibrational excitation of N_2 as a function of electric field (E_0) for 70, 80, 90 and 100 km. Blue solid line: Non-Maxwellian. Blue dashed-dotted line: Maxwellian at the electron temperature T_{2nd}. Red solid line: T_{2nd} as a function of electric field.

in the gradient temperature T_{eff} around 0.5-1.5 eV, particularly around 1.1 eV, and to a second moment temperature T_{2nd} that varies depending on the strength of the electric field. The temperature T_{2nd} increases sharply for electric fields above 2 V/m, resulting in a relatively high T_{2nd}. The aforementioned effects cause the non-Maxwellian Q to be lower than the Maxwellian Q for electric fields above 2 V/m due to the more pronounced cut-off at 2 eV. This leads to reductions in electron energy losses to vibrational excitation of N_2 for electrons with energies above 2 eV compared to a Maxwellian distribution. Provided that the electron gas absorb a constant amount of heat, other cooling processes must increase to balances constant electron heating rates at steady state. As shown in paper I, this is caused by increases in phase space densities below 2 eV. Additionally, the Maxwellian is computed at the relatively high second moment temperature of the non-Maxwellian, and a Maxwellian distribution at this temperature will have much larger cooling rates balancing a significantly larger heating rate. This means that the non-Maxwellian and Maxwellian Q correspond to two different energy flow through the electron gas. Below electric

https://doi.org/10.5194/egusphere-2026-1118
Preprint. Discussion started: 27 March 2026

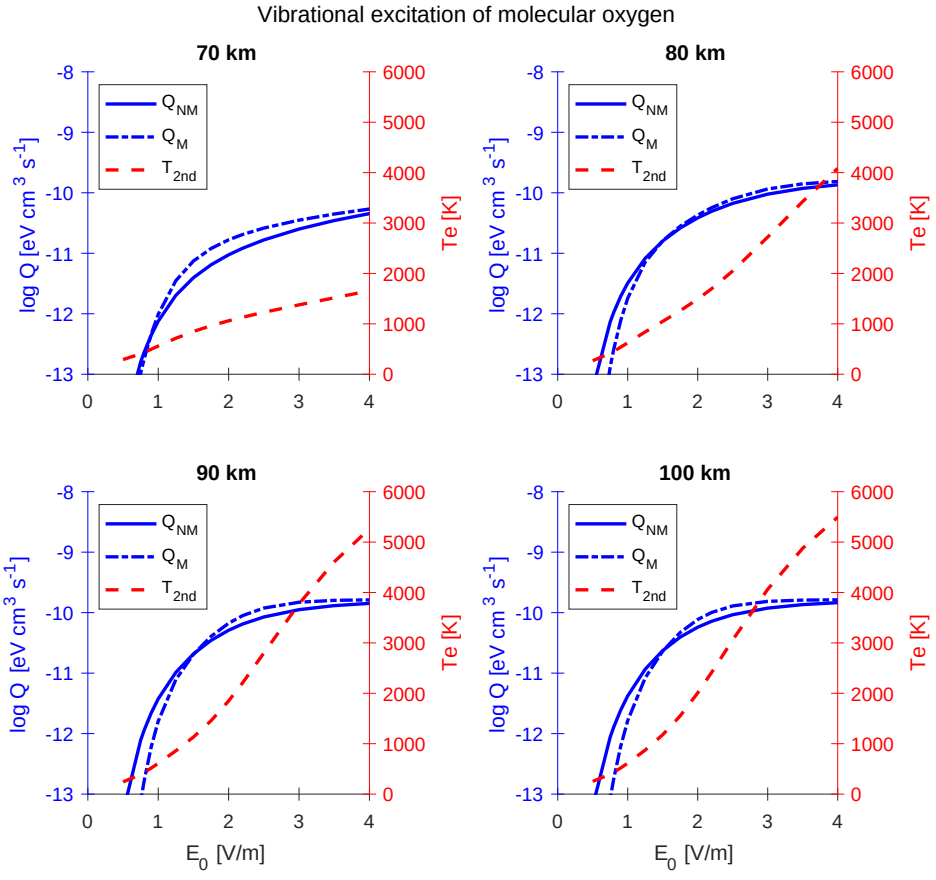

Figure 2. $\log_{10} Q$ for vibrational excitation of O_2 as a function of electric field (E_0) for 70, 80, 90 and 100 km. Blue solid line: Non-Maxwellian. Blue dashed-dotted line: Maxwellian at the electron temperature T_{2nd}. Red solid line: T_{2nd} as a function of electric field.

fields of 2.0 V/m, the non-Maxwellian Q is higher than the Maxwellian because the cut-off is less pronounced. This means that the energy loss of electrons above 2.0 eV is less significant. A less pronounced cut-off means that fewer electrons have degraded from energies above 2 eV to lower energies, leading to a comparably lower temperature T_{2nd}. Consequently, the Maxwellian cooling rates are computed at this comparably lower temperature, making the Maxwellian cooling rates appear lower than the non-Maxwellian rates.

For vibrational excitation of O_2, the non-Maxwellian and Maxwellian cooling rates are quite similar. In regions where the cross section of vibrational excitation of O_2 is large (0.3-1.1 eV), the phase space density of the non-Maxwellian and Maxwellian distribution are relatively similar, although the non-Maxwellian phase space density exhibits a slightly steeper decrease, as shown in Paper I. Below electric fields of 1 V/m, the non-Maxwellian cooling rates for O_2 are slightly higher than the Maxwellian rates, which likely follow the same explanation as for N_2, where the Maxwellian cooling rates are computed at a comparably lower temperature. The reason why the cooling rates for excitation of fine structure levels in O are higher for the

https://doi.org/10.5194/egusphere-2026-1118
Preprint. Discussion started: 27 March 2026

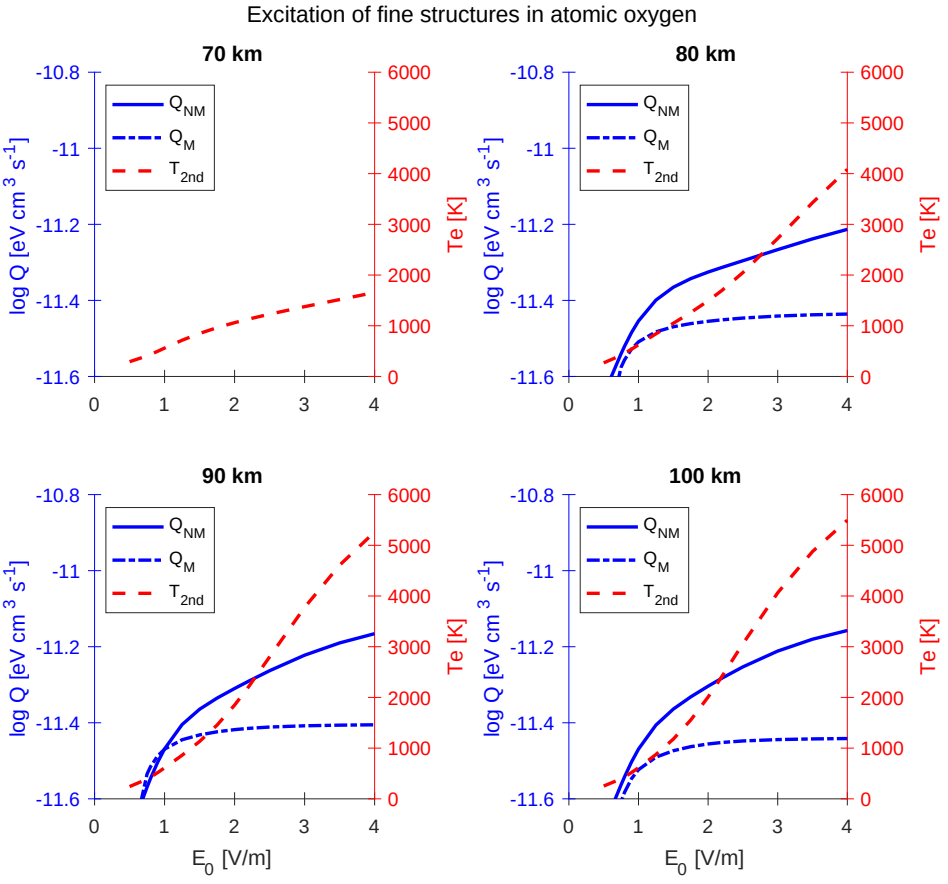

Figure 3. $\log_{10} Q$ for excitation of fine structure levels in O as a function of electric field (E_0) for 70, 80, 90 and 100 km. Blue solid line: Non-Maxwellian. Blue dashed-dotted line: Maxwellian at the electron temperature $T_{2\mathrm{nd}}$. Red solid line: $T_{2\mathrm{nd}}$ as a function of electric field.

non-Maxwellian compared to the Maxwellian is due to the large cross sections in the regions where electrons are redistributed by vibrational excitation of N_2 to around 1.0-1.5 eV and by vibrational excitation of O_2 to energies around 0.1 eV.

This show that a Maxwellian distribution with a temperature corresponding to the second moment temperature of hot non-Maxwellian distributions leads to unreasonably high electron cooling. From an energetics perspective, this means that a Maxwellian at $T_{2\mathrm{nd}}$ is not consistent with the heat absorbed by the non-Maxwellian gas. If we instead use a Maxwellian distribution that has the same absorbed energy as the corresponding non-Maxwellian, the resulting Maxwellian has a much lower temperature T_{L} (ref. Eq. 5). Hence, the heated non-Maxwellian distribution contains more total thermal energy than the Maxwellian distribution that loses the same amount of energy to cooling processes. Figure 4 shows the ratio between total cooling rates for a Maxwellian at $T_{2\mathrm{nd}}$ and the total non-Maxwellian cooling rates in panel (a) and the ratio between $T_{2\mathrm{nd}}$ and T_{L} in panel (b). Panel (c) and (d) show total cooling rates for a Maxwellian at $T_{2\mathrm{nd}}$, a non-Maxwellian and a Maxwellian at

https://doi.org/10.5194/egusphere-2026-1118
Preprint. Discussion started: 27 March 2026

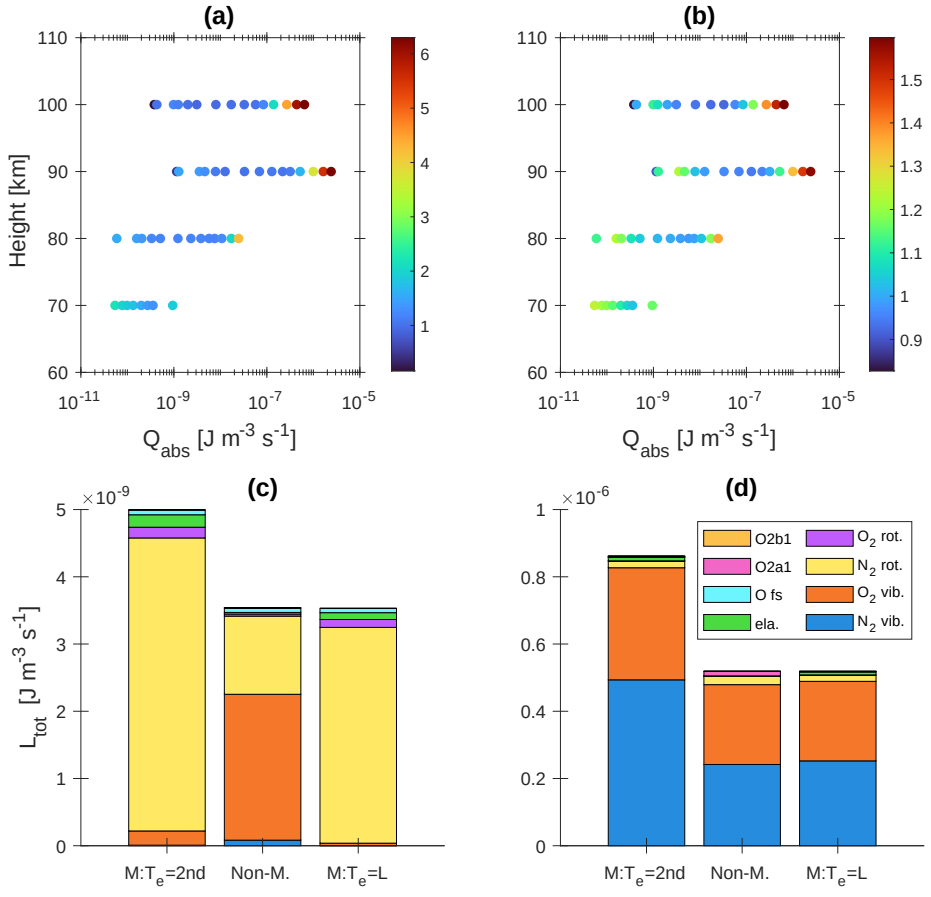

Figure 4. Panel **(a)**: Ratio $L_{\mathrm{M}}/L_{\mathrm{NM}}$ between total cooling rates for a Maxwellian at $T_{2\mathrm{nd}}$ and total non-Maxwellian cooling rates. Panel **(b)**: Ratio $T_{2\mathrm{nd}}/T_{\mathrm{L}}$. For both panel (a) and (b), the x-axis show the total absorbed power Q_{abs} for the non-Maxwellian electron gas. Panel **(c)**: Total cooling rates for Maxwellian at $T_{2\mathrm{nd}}$, non-Maxwellian and Maxwellian at T_{L} for $E_0 = 0.75$ V/m. Panel **(d)**: Same as panel (c), but $E_0 = 2.5$ V/m.

T_{L} with $E_0 = 0.75$ V/m and $E_0 = 2.5$ V/m, respectively. This figure illustrate that the total cooling rates for a Maxwellian at $T_{2\mathrm{nd}}$ become unreasonably high when the non-Maxwellian have a large total thermal energy. Therefore, in Fig. 5, Fig. 6 and Fig. 7, we show electron cooling rates Q, which are the same as Fig. 1, Fig. 2 and Fig. 3, but with a Maxwellian at the electron temperature T_{L}. Overall, the temperature T_{L} is lower than $T_{2\mathrm{nd}}$, especially at 90 and 100 km, where $T_{2\mathrm{nd}}$ exceeds 5000 K while T_{L} remain below 3500 K. The cooling rates for non-Maxwellian and Maxwellian at T_{L} for both vibrational excitation of N_2 and O_2 in Fig. 5 and Fig. 6, respectively, appear more reasonable for the hot non-Maxwellian case. Here, a Maxwellian at T_{L} seems to be a better measure than a Maxwellian at $T_{2\mathrm{nd}}$. However, the cooling rates for a Maxwellian at T_{L} are generally lower for the colder non-Maxwellian case. This is likely caused by the inclusion of too few transitions for rotational excitation N_2 and O_2, as well as outdated cross sections for elastic collisions, as shown in panel (c) of Fig. 4.

https://doi.org/10.5194/egusphere-2026-1118
Preprint. Discussion started: 27 March 2026

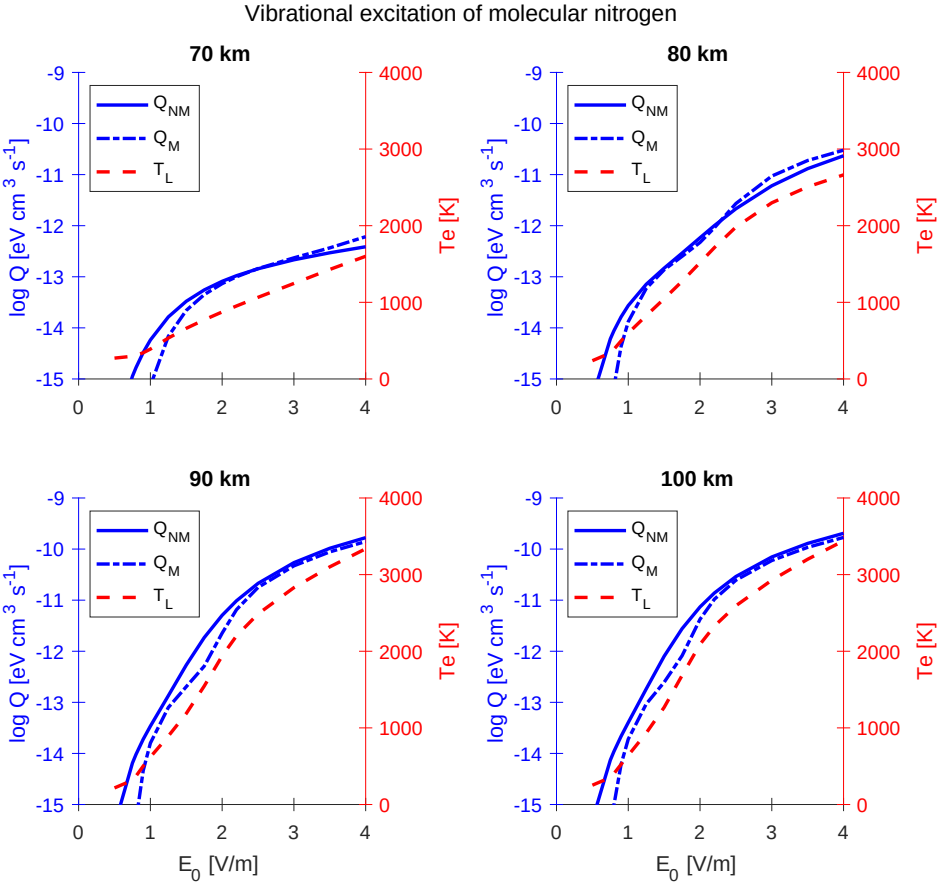

Figure 5. $\log_{10} Q$ for vibrational excitation of N_2 as a function of electric field (E_0) for 70, 80, 90 and 100 km. Blue solid line: Non-Maxwellian. Blue dashed-dotted line: Maxwellian at the electron temperature T_L. Red solid line: T_L as a function of electric field.

4 Discussion

One important difference between the non-Maxwellian and Maxwellian cooling rates is that the Maxwellian cooling rates are uniquely controlled by the electron temperature. In contrast, for the non-Maxwellian distribution, the cooling rates depend on the shape of the distribution, which is not uniquely determined by its second moment but also influenced by the impact of inelastic collisions with the neutral atmosphere. Previous studies typically provide analytical expression for the cooling rates as a function of electron temperature. These are usually derived and computed from expressions such as Eq. 2 and 8, assuming a Maxwellian distribution. For example, for ionospheric modelling of radio wave propagation through the D region ionosphere, one can use the simplified electron energy equation from Eq. 5, where analytical expressions are often applied for the total Maxwellian electron cooling rates. The balance between local heating and cooling determines the electron temperature, which in turn determines the electron cooling rates. The non-Maxwellian cooling rates, on the other hand, arises as a by-product

https://doi.org/10.5194/egusphere-2026-1118
Preprint. Discussion started: 27 March 2026

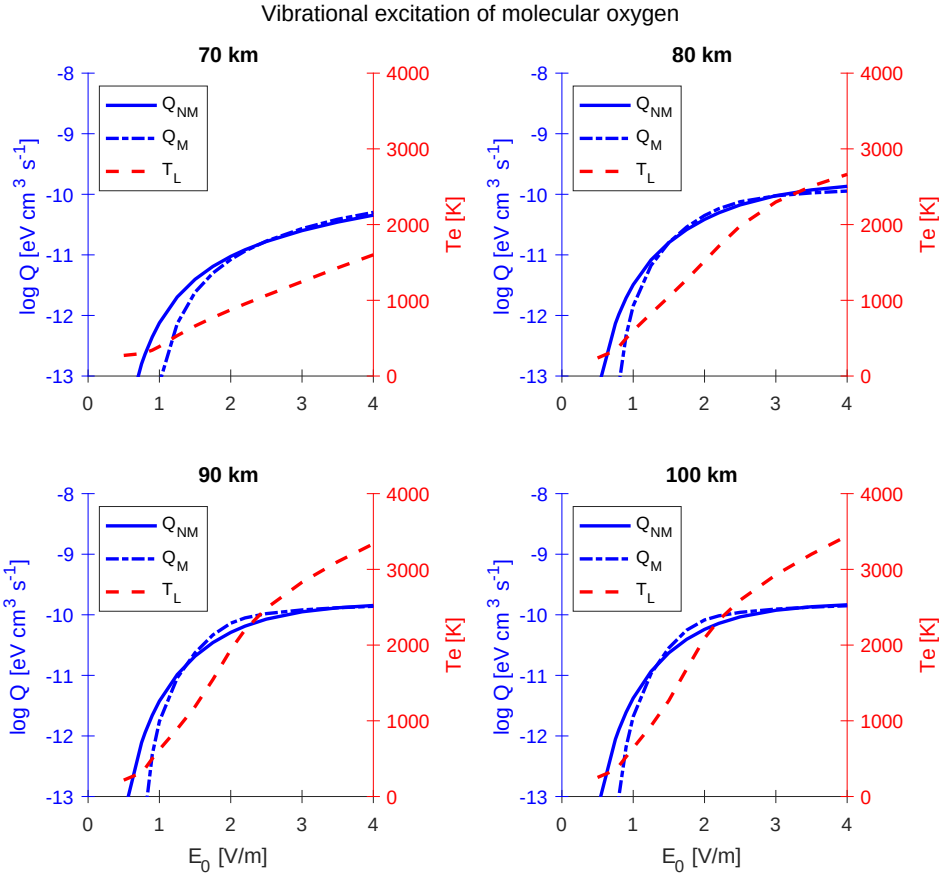

Figure 6. $\log_{10} Q$ for vibrational excitation of O_2 as a function of electric field (E_0) for 70, 80, 90 and 100 km. Blue solid line: Non-Maxwellian. Blue dashed-dotted line: Maxwellian at the electron temperature T_L. Red solid line: T_L as a function of electric field.

of the calculation of the distribution function described in paper I. The distribution function is governed by the heat added to the electron gas and energy loss processes due to inelastic collisions. Macroscopic properties of the electron gas, such as electron temperature and electron cooling rates, can be computed through integrals over the electron distribution function. Our solution of Boltzmann equation provides both the second moment temperatures and the cooling rates. However, since the second moment electron temperature does not uniquely specifies the distribution function, it is insufficient to compute the electron cooling rates.

During strong radio wave heating, our results show that the electron distribution becomes significantly different from a Maxwellian distribution. At steady state, the non-Maxwellian distribution does not change over time because the electrons lose as much energy as is added through the HF heating wave. For this modified non-Maxwellian distribution, different inelastic collision dominate compared to a Maxwellian, primarily due to the cut-off at 2.0 eV, where electrons degrade to lower energies

https://doi.org/10.5194/egusphere-2026-1118
Preprint. Discussion started: 27 March 2026

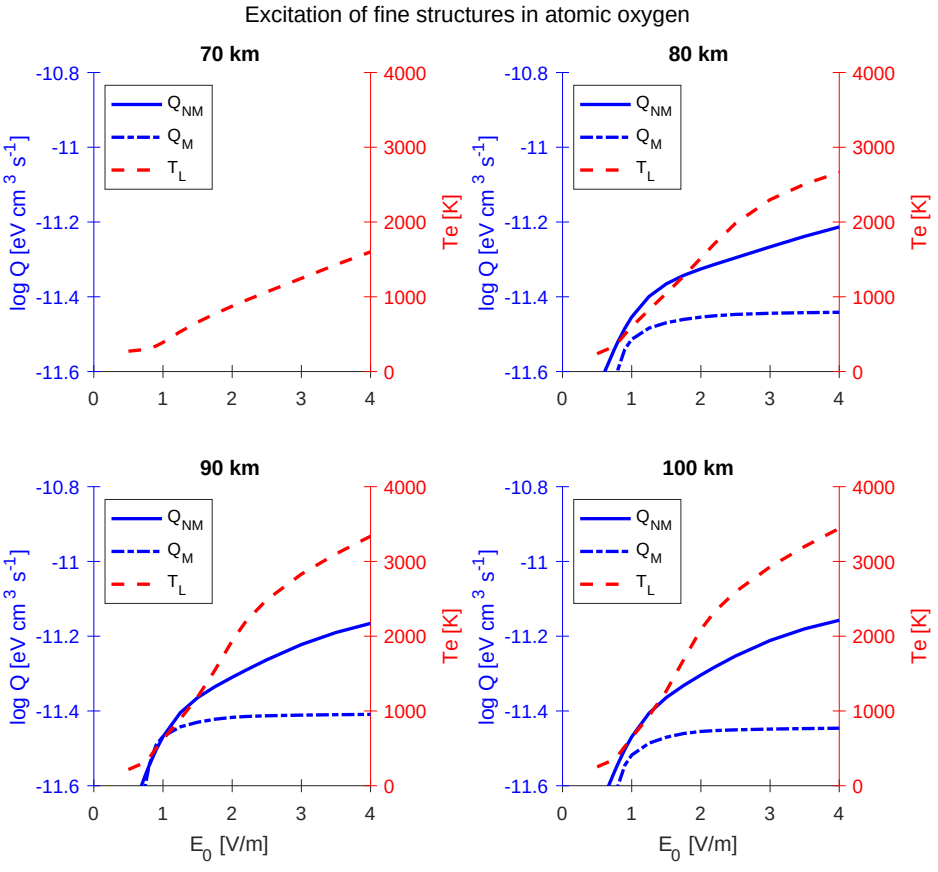

Figure 7. $\log_{10} Q$ for excitation of fine structure levels in O as a function of electric field (E_0) for 70, 80, 90 and 100 km. Blue solid line: Non-Maxwellian. Blue dashed-dotted line: Maxwellian at the electron temperature T_L. Red solid line: T_L as a function of electric field.

since the number of electrons has to be conserved. This causes the non-Maxwellian electrons to lose less energy to N_2 through vibrational excitation, and more to O through excitation of fine structure levels.

The results in this paper are somewhat similar to modelling by Milikh and Dimant (2003), who studied frictional electron heating in the E region auroral electrojet during magnetic storms. Milikh and Dimant (2003) found that the non-Maxwellian cooling rates are lower than the Maxwellian cooling rates for the temperatures they observed. The main difference between the work in this paper and Milikh and Dimant (2003) is that they model the electron distribution function at E region height with a turbulent electric field parallel to the magnetic field to represent frictional heating, while this work apply an oscillating electric field perpendicular to the magnetic field to represent HF radio wave heating in the D region. This corresponds to approximately three orders of difference in neutral density and one order of difference in electron density. However, qualitatively our results are consistent.

https://doi.org/10.5194/egusphere-2026-1118
Preprint. Discussion started: 27 March 2026

The cooling rate modification discussed in this paper should be applicable to any scenario where the electron gas in the lower ionosphere is significantly heated, since the HF radio primarily add heat to the electron gas through Omhic heating, while the phase space density remain isotropic. As a consequence, the results presented in this paper utilized to model the response of the D region to any natural physical processes that add heat to the electron gas. One example is large enough frictional heating due to ExB-drift, which can heat the electron temperature to as much as three times the background neutral temperature (Browner et al., 2009). Browner et al. (2009) argues that, since the temperature enhancement is moderate and the ExB drift velocity is smaller than the thermal velocity, the velocity distribution does not deviate significantly from a Maxwellian. Therefore, they justify the use of Maxwellian cooling rates. This contrast with our results, which are non-Maxwellian mainly due to N_2 cut-off, which become more pronounced with higher energy input (i.e. higher temperature). Even for temperatures as low as 600-700 K, the tail of the electron distribution deviates from a Maxwellian, as demonstrated in Paper I. The remaining question is at what temperature the deviation from a Maxwellian becomes important enough to take into account. To our understanding, this ought to be more important in the upper part of the D region and the lower part of the E region.

Even though heating works differently in the D region and E-region, any natural process that increases the heat input in the E-region will behave similarly to the D region. This might indicate that the cooling rates for the D region during heating, as presented in this paper, might have implications for cooling rates in the E-region, if heating or any natural processes increases the temperature to a sufficiently high level, provided that the difference in neutral density is taken into account.

5 Conclusions

This paper demonstrates that deviations from a Maxwellian influence the macroscopic properties of the electron gas, such as electron cooling rates. The vibrational excitation of molecular nitrogen and oxygen, as well as the excitation of fine structure levels in atomic oxygen, differ from Maxwellian cooling rates. Inelastic collisions between electrons and neutrals lead to excitation of different states in the neutrals, causing a redistribution of electrons. Cooling rates are determined by integrating over the phase space density, multiplied by cross sections and energy. Any changes in the phase space density will, therefore, affect the cooling rates. If the cross section of any inelastic collision process happens to be large in regions with increased phase space density, this will results in an increase in the cooling rates, as observed in the excitation of fine structure levels in O. Conversely, vibrational excitation of N_2 has large cross sections in regions with reduced phase space density, i.e. above approximately 2.0 eV. During strong radio wave heating, these cooling rates are reduced. Cooling rates for vibrational excitation of O_2 remain comparable to Maxwellian rates because their cross section are large in energy ranges where the phase space density is quite similar to a Maxwellian.

Code and data availability. Code and data computing cooling rates will be made available.

https://doi.org/10.5194/egusphere-2026-1118
Preprint. Discussion started: 27 March 2026

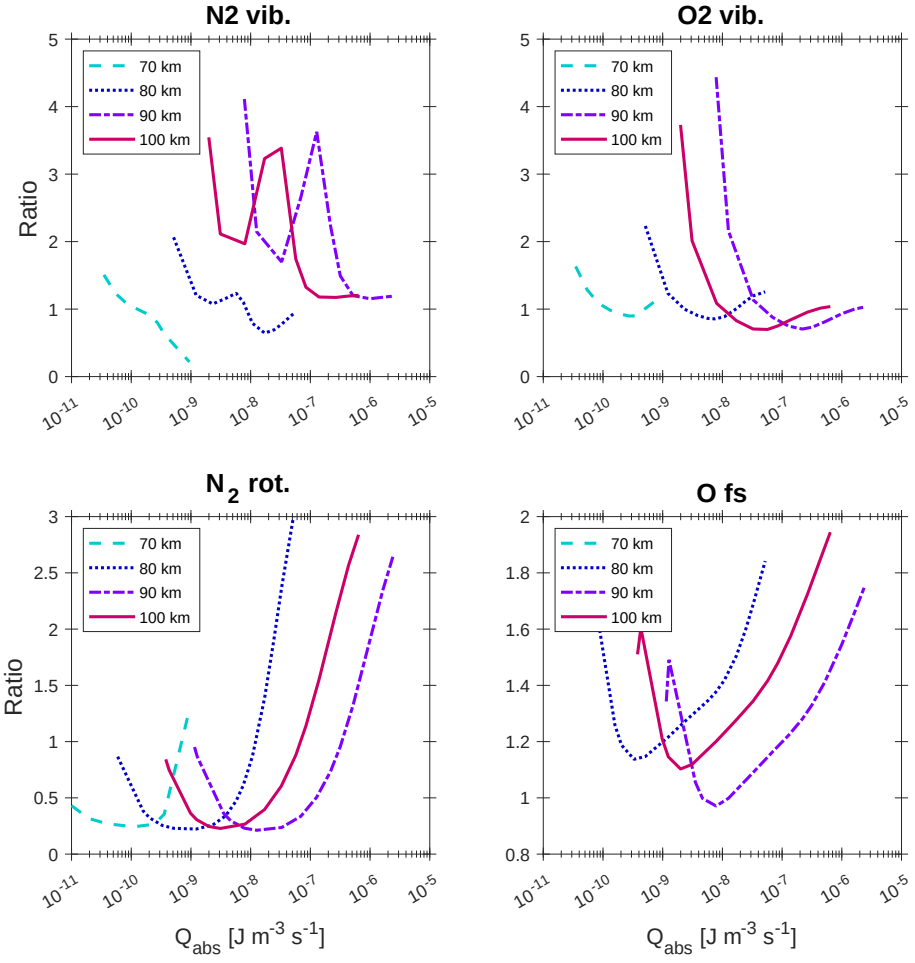

Figure A1. Ratio of Q for non-Maxwellian and Maxwellian at T_{L} as a function of the absorbed power Q_{abs} of the non-Maxwellian electron gas. The different panels show ratios for vibrational excitation of N_2, vibrational excitation of O_2, rotational excitation of N_2 and excitation of fine structure levels in O.

Appendix A: Correction factor for Maxwellian cooling rates

Figure A1 presents correction factors that take into account the deviation from a Maxwellian. These correction factors are shown as a function of the absorbed power of the non-Maxwellian electron gas, which is found from Eq. 5, i.e the absorbed power is equal to the sum of the total cooling rates. The absorbed power at each height and electric field have a corresponding second moment temperature for the non-Maxwellian. We present the correction factors in Fig. A1 as the ratio between non-Maxwellian and Maxwellian cooling rates, where the Maxwellian is at the temperature T_{L}. The different panels in Fig. A1 show the ratio for vibrational excitation of N_2, vibrational excitation of O_2, rotational excitation of N_2 and excitation of fine structure levels in O.

https://doi.org/10.5194/egusphere-2026-1118
Preprint. Discussion started: 27 March 2026

Author contributions. MM made the program computing electron cooling rates and prepared the initial manuscript. BG suggested the topic and supervised the project. All authors contributed to the preparation of the manuscript.

Competing interests. No competing interest to declare.

Acknowledgements. We would like to thank ChatUiT for grammatical improvements.

https://doi.org/10.5194/egusphere-2026-1118
Preprint. Discussion started: 27 March 2026

References

Allen, A.: Measurements of absolute differential cross sections for vibrational excitation of O_2 by electron impact, J. Phys. B: At. Mol. Opt. Phys., 28 5163, 1995.

Baumann, C., Rapp, M., Kero, A., and Enell, C.-F.: Meteor smoke influence on the D-region charge balance –review of recent in situ measurements and one-dimensional model results, Ann. Geophys., 31, 2049–2062, https://doi.org/10.5194/angeo-31-2049-2013, 2013.

Bell, K. L., Berrington, K. A., and Thomas, M. R. J.: Electron impact excitation of the ground-state ^3P fine-structure levels in atomic oxygen, Mon. Not. R. Astron. Soc., L83-L87, 293, 1998.

Belova, E. G., Pashin, A. B., and Lyatsky, W. B.: Passage of a powerful HF radio wave through the lower ionosphere as a function of initial electron density profiles, Journal of Atmospheric and Terrestrial Physics, 57, 265–272, https://doi.org/10.1016/0021-9169(93)E0012-X, 1995.

Browner, L., Thayer, J. P., and St-Marice, J. P.: Frictionally heated electrons in the high-latitude D region, Journal of geophysical research, 114, A12302, https://doi.org/10.1029/2009JA014421, 2009.

Campbell, L., Brunger, M., Cartwright, D., and Teubner, P.: Production of vibrationally excited N_2 by electron impact, Planetary and Space Science, 52, 815–822, 2004.

Carleton, N. P. and Megill, L. R.: Electron energy distribution in slightly ionized air under the influence of electric and magnetic fields, Phys. Rev., 126, 2089–2099, 1962.

Gurevich, A. V.: Nonlinear phenomena in the Ionosphere, Springer-Verlag, New York, ISBN 0387086056, 1978.

Gustavsson, B., Sergienko, T., Haggestrom, I., Honary, F., and Aso, T.: Simulation of high energy tail of electron distribution function, Adv. Polar Upper Atmos. Res., 18, 1–9, 2004.

Gustavsson, B., Rietveld, M. T., Ivchenko, N. V., and Kosch, M. J.: Rise and fall of electron temperature: Ohmic heating of ionospheric electrons from underdense HF radio wave pumping, Journal of Geophysical Research, 115, A12332, https://doi.org/10.1029/2010JA015873, 2010.

Hansen, J. D., Morales, G. J., and Magges, J. E.: Large-Scale HF-Induced Ionospheric Modifications: Theory and Modeling, Journal of Geophysical Research, 97, No. A11, 17,019–17,032, 1992.

Hedin, A. E.: Extension of the MSIS thermosphere model into the middle and lower atmosphere, J. Geophys. Res., 96, 1159–1172, 1991.

Itikawa, Y., Hayashi, M., Ichimura, A., Onda, K., Sakimoto, K., Takayanagi, K., Nakamura, M., Nishimura, H., and Takayanagi, T.: Cross Sections for Collisions of Electrons and Photons with Nitrogen Molecules, Journal of Physical and Chemical Reference Data, 15, https://doi.org/10.1063/1.555762, 1986.

Itikawa, Y., Hayashi, M., Ichimura, A., Onda, K., Sakimoto, D., Takayanagi, K., Nakamura, M., Nishimura, H., and Takayanagi, T.: J. Phys. Chem. Ref. Data, J. Phys. Chem. Ref. Data, 35, 31, 2006.

Jones, D. B., Campbell1, L., Bottema, M. J., and Brunger, M. J.: New electron-energy transfer rates for vibrational excitation of O_2, New Journal of Physics, 114, 5, 2003.

Kassa, M., Havnes, O., and Belova, E.: The effect of electron bite-outs on artificial electron heating and the PMSE overshoot, Ann. Geophys., 23, 3633–3643, https://doi.org/10.5194/angeo-23-3633-2005, 2005.

Kero, A., Bösinger, T., Pollari, P., Turunen, E., and Rietveld, M.: First EISCAT measurements of electron-gas temperature in the artificially heated D-region ionosphere, Ann. Geophys., 18, 1210–1215, https://doi.org/10.1007/s00585-000-1210-8, 2000.

https://doi.org/10.5194/egusphere-2026-1118
Preprint. Discussion started: 27 March 2026

Kero, A., Enell, C. F., Ulich, T., Turunen, E., Rietveld, M. T., and Honary, F. H.: Statistical signature of active D-region HF heating in IRIS riometer data from 1994-2004, Ann. Geophys., 25, 407–415, https://doi.org/10.5194/angeo-25-407-2007, 2007.

Milikh, G. M. and Dimant, Y. S.: Model of anomalous electron heating in the E region: 2. Detailed numerical modeling, J. Geophys. Res., 108 (A9),1351, https://doi.org/10.1029/2002JA009527, 2003.

Mintzer, D.: Transport theory of gases, in The Mathematics of Physics and Chemistry, edited by H. Margenau and G. M. Murphy, Von Nostrand Reinhold Company, New York, vol. 2 edn., 1964.

Myrvang, M., Baumann, C., and Mann, I.: Modelling the influence of meteoric smoke particles on artificial heating in the D-region, Ann. Geophys., 39, 1055–1068, https://doi.org/10.5194/angeo-39-1055-2021, 2021.

Pavlov, A. V.: New electron energy transfer rates for vibrational excitation of N_2, Ann. Geophys., 16, 176–182, 1998a.

Pavlov, A. V.: New electron energy transfer and cooling rates for vibrational excitation of O_2, Ann. Geophys., 16, 1007–1013, 1998b.

Pavlov, A. V. and Berringston, K. A.: Cooling rates of thermal electrons by electron impact excitation of fine structure levels of atomic oxygen, Ann. Geophys., 17, 919–924, 1999.

Picone, J., Hedin, A., Drob, D., and Aikin, A.: NRLMSISE-00 empirical model of the atmosphere: Statistical comparisons and scientific issues, J. Geophys. Res., 107(A12), 1468, https://doi.org/10.1029/2002JA009430, 2002.

Rees, M. H.: Physics and chemistry of the upper atmosphere, Cambrigde University Press, Trumpington Street, Cambrige, United Kingdom, ISBN 0-521-32305-3, 1989.

Schmalzried, A., Luque, A., and Lehtinen, N.: IAA Database on lxcat, www.lxcat.net/IAA, [data set], 2023.

Schunk, R. W. and Nagy, A. F.: Electron temperature in the F-region of the ionosphere: Theory and observations, Rev. Geophys., 16, 355–399, 1978.

Shoucri, M. M. and Morales, G. J.: Ohmic Heating of the Polar F Region by HF Pulses, Journal of geophysical research, 89, 2907–2917, 1984.

Stubbe, P.: Modyfing effects of a strong electromagnetic wave upon a weakly ionized plasma: A kinetic description, Radio Science, 16, 417–421, 1981.

Stubbe, P. and Varnum, W. S.: Electron energy transfer rates in the ionosphere, Space Sci., 20, 1121–11 261, 1972.

Takayanagi, K. and Itikawa, Y.: The rotational excitation of molecules by slow electrons, in: Advances in Atomic and Molecular Physics, vol. 6, pp. 105–153, Elsevier, 1970.